# Decoupled Holocene variability in surface and thermocline water temperatures of the Indo-Pacific Warm Pool

Haowen Dang,[1] Zhimin Jian,[1] Franck Bassinot,[2] Peijun Qiao,[1] and Xinrong Cheng[1]

Received 15 November 2011; accepted 29 November 2011; published 4 January 2012.

[1] The Holocene variability in sea surface and thermocline water temperatures (SST and TWT) in the Indo-Pacific Warm Pool (IPWP) has been reconstructed by planktonic foraminiferal Mg/Ca from sediments of the western tropical Philippine Sea. Afterward the Younger Dryas interval (YD), SST warmed gradually till ∼10 ka and remained approximately constant afterwards, but TWT rose more rapidly to a peak between ∼12 and ∼10 ka and then declined by ∼1.5°C through the Holocene. The trend of TWT closely followed the boreal summer insolation and could be correlated to tropical climate changes represented by southward movement of the Inter-tropical Convergence Zone (ITCZ) and related changes in East Asian monsoons.
**Citation:** Dang, H., Z. Jian, F. Bassinot, P. Qiao, and X. Cheng (2012), Decoupled Holocene variability in surface and thermocline water temperatures of the Indo-Pacific Warm Pool, *Geophys. Res. Lett.*, *39*, L01701, doi:10.1029/2011GL050154.

## 1. Introduction

[2] Knowledge of Holocene climate variability is of essential importance for our understanding of the Earth's internal climatic feedbacks since the response of the climate system to solar forcing can be examined under relatively stable climate backgrounds (i.e., ice volume, vegetation cover, greenhouse gas levels, etc.). Previous studies have demonstrated a general scenario for the Northern Hemisphere that includes an Early Holocene Optimum and gradual changes afterwards which generally followed the boreal summer insolation [e.g., *Haug et al.*, 2001; *Wang et al.*, 2005].

[3] An understanding of Holocene climatic changes in the IPWP would appear to be critical due to the substantial export of heat and water vapor from this region to the rest of the globe. However, previous SST reconstructions in the IPWP revealed a very weak cooling that could hardly linearly match the fundamental decrease in boreal summer insolation [e.g., *Stott et al.*, 2004; *Linsley et al.*, 2010]. Such a discrepancy indicates that additional processes besides SST may be involved into the climatic mechanism of the IPWP. In this regard, an understanding of processes operative within the tropical thermocline may be important, not only because of its role in basin-scale water mass exchange and thereby potential to convey remote climate signals [e.g., *Luyten et al.*, 1983; *Liu et al.*, 1994; *Qu et al.*, 1999; *Harper*, 2000], but also due to its capacity to modulate SST and climate by changing the storage and distribution of heat in the mixed layer [e.g., *Chen et al.*, 1994; *Seager and Murtugudde*, 1997].

[4] Here, the Holocene SST and TWT of the western tropical Pacific are reconstructed using planktonic foraminifera proxies. Our results allow examinations of past thermal conditions in the IPWP thermocline and assessments of the role these conditions played in Holocene climate changes.

## 2. Oceanographic Setting

[5] The western Philippine Sea is a water mass crossroad in the tropical Pacific. Relatively saline North Pacific Tropical Water (NPTW, salinity typically >34.75 psu, [*Qu et al.*, 1999]) (Figures 1a and 1b) is mainly found at depths around 50∼300 m and is thought to be brought in by the North Equatorial Current (NEC) from where it is formed in the central Pacific (10°–25°N, 140°E–160°W) by evaporation and subduction of mid-latitude surface waters [*Fine et al.*, 1994, 2001]. Above that level, the warm Tropical Surface Water (TSW, typically warmer than 26°C) from the IPWP largely controls the near-surface (<50 m) in the study region [*Qu et al.*, 1999] (Figure 1b).

[6] In the tropical Pacific, ventilation of the thermocline, which is mainly driven by the subduction of warm and saline sub-tropical waters in the mid-latitude basin center and occurs on a decadal travel time, is crucial for connecting the tropical and subtropical circulations [e.g., *Fine et al.*, 1994, 2001; *Huang and Liu*, 1999; *Harper*, 2000]. It was suggested that "a potential vorticity barrier that inhibits the direct flow of lower-layer water from the subtropical north Pacific to the equator" could be created by ITCZ [*Lu and McCreary*, 1995].

[7] At the site of our study, the upper ocean circulation is greatly affected by the shift of the NEC's bifurcation latitude (NECB). Thanks to the local wind curl, the NECB is shifted northward (∼15°N) by the East Asian winter monsoon (EAWM) and southward (∼12°N) by the summer monsoon (EASM), and can be shifted to higher latitudes by El Niño [e.g., *Qu and Lukas*, 2003; *Kim et al.*, 2004].

## 3. Material and Methods

### 3.1. Core MD98-2188

[8] A large-diameter CALYPSO core, MD98-2188 (14.82°N; 123.49°E; 730 m water depth, see Figure 1a for core location) was recovered offshore Luzon during the IMAGES IV cruise (see Data Set S1 in the auxiliary material).[1] The upper 3.94 m of the core (total length: 16.3 m) revealed undisturbed light brownish clay. The age model for this upper section was established based on a series

[1]State Key Laboratory of Marine Geology, Tongji University, Shanghai, China.
[2]Laboratoire des Science du Climat et de l'Environnement, Domaine du CNRS, Gif-sur-Yvette, France.


0094-8276/12/2011GL050154

[1]Auxiliary materials are available at ftp://ftp.agu.org/apend/gl/2011gl050154.

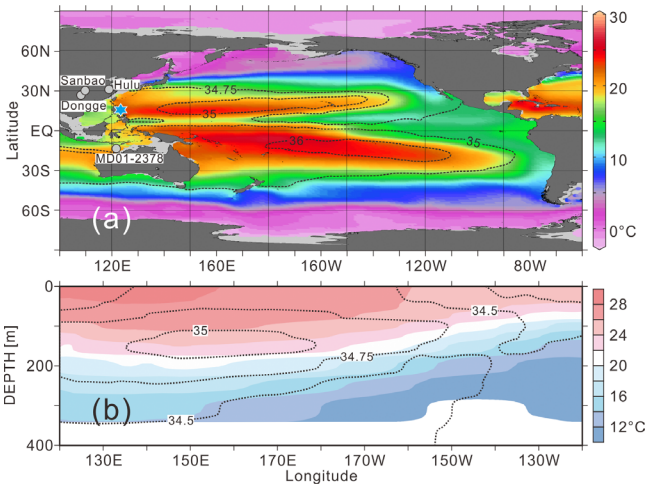


**Figure 1.** Map-view and cross-section of the Pacific showing subsurface temperature-salinity structures. (a) Temperature (color shading) and salinity (contours) at 150 m water depth, color scale for temperature is shown at the right, dashed contours denote 34.75, 35 and 36 psu isohalines, respectively. (b) 15°N cross-section of temperature (shading) and salinity (contours) down to 400 m water depth, color scale for the 2°C contour interval temperature shading is shown at the right, dotted lines are isohalines with 0.25 psu contour interval. Data from WOA09 [*Locarnini et al.*, 2010; *Antonov et al.*, 2010]. The location of MD98-2188 is marked as a blue hexagram, and the locations of Chinese stalagmite records from Hulu, Sanbao and Dongge caves [*Wang et al.*, 2001, 2005, 2008] and marine sediment core MD01-2378 [*Xu et al.*, 2006, 2008] in IPWP are marked by grey dots in Figure 1a.

of 5 planktonic foraminifera AMS $^{14}$C dates [*Lin et al.*, 2006] that were converted to calendar ages using CALIB 5.0 [*Stuiver and Reimer*, 1993] and a 400-year reservoir correction. The average sedimentation rate of core MD98-2188 is 30.3 cm/kyr (18.7∼57.2 cm/kyr), equivalent to an average time resolution of ∼66 yrs (35∼110 yrs) for the 2 cm sampling interval (Figure 2g).

### 3.2. Oxygen Isotope and Mg/Ca Measurements

[9] Specimens of the surface-dwelling *Globigerinoides ruber* s.s. (white) and the deeper, thermocline-dwelling *Pulleniatina obliquiloculata* (depth habitats discussed in section 3.3) were hand-picked from 300∼360 $\mu$m and 360∼440 $\mu$m size fractions, respectively, for the isotopic analysis. The oxygen isotope analysis followed the method described by *Cheng et al.* [2005], with a standard deviation of 0.07‰ PDB (1$\sigma$) [*Cheng et al.*, 2005].

[10] For the Mg/Ca analysis, *G. ruber* and *P. obliquiloculata* were hand-picked from 250∼350 $\mu$m and 360∼440 $\mu$m size fractions, respectively. Specimens were pretreated and cleaned with a reductive step [*Martin and Lea*, 2002] and were measured on an ICP-AES. For the Mg/Ca-temperature calculations, equations given by *Anand et al.* [2003] (SST = ln (Mg/Ca$_{G.\ ruber}$ ÷ 0.38)/0.09, TWT = ln (Mg/Ca$_{P.\ obliquiloculata}$ ÷ 0.328)/0.09, non-reductive cleaning protocol) were utilized since they give more comparable core top results to modern atlas than other calibrations using a reductive step [e.g., *Lea et al.*, 2000], in spite of the probable underestimation of temperature results as suggested by some inter-calibration studies [e.g. *Rosenthal et al.*, 2004; *Xu et al.*, 2008]. The overestimated temperatures when using the equations of *Lea et al.* [2000] may have resulted from less dissolution at the shallower water depth of MD98-2188 than accounted for in the *Lea et al.* [2000] calibration. Hence, although potential bias might exist in the absolute value of the estimated temperature, our Mg/Ca results are expected to be valid representations of thermal conditions in the region, especially with regard to past variability. The average reproducibilities of Mg/Ca for *G. ruber* (13 replicates) and *P. obliquiloculata* (21 replicates) were 1.8% and 5.2% (1$\sigma$), equivalent to ±0.2°C and ±0.5°C (1$\sigma$), respectively.

[11] The difference between parallel-measured SST and TWT ($\Delta T_{G\text{-}P}$) is taken as a proxy for upper-ocean thermal-gradient. The $\delta^{18}$O of seawater ($\delta^{18}O_{sw}$) is calculated from $\delta^{18}$O of *G. ruber* [*Bemis et al.*, 1998] subtracting the Mg/Ca-SST and mean sea level [*Waelbroeck et al.*, 2002].

### 3.3. Core-Top Examination on the Depth Habitats of *G. ruber* and *P. obliquiloculata*

[12] *G. ruber* and *P. obliquiloculata* are usually considered to be typical tropical species that live within and

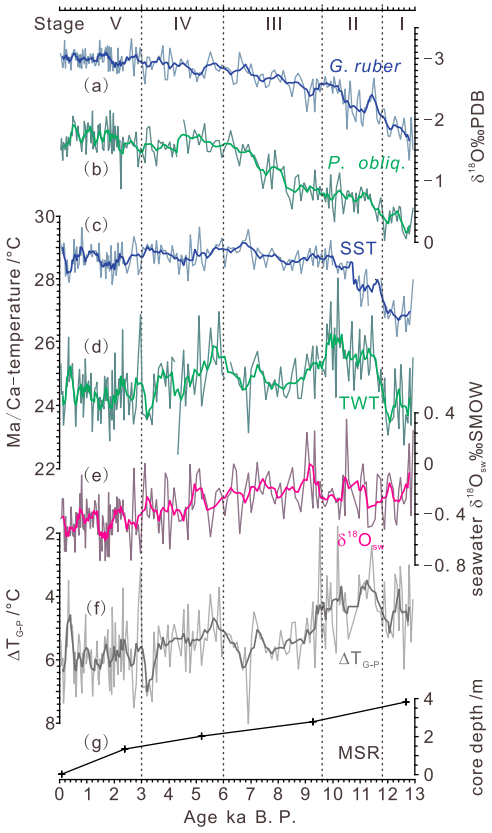


**Figure 2.** Reconstructed planktonic foraminiferal proxy records for core MD98-2188: (a and c) $\delta^{18}$O and Mg/Ca temperature for *G. ruber* (blue) and (b and d) *P. obliquiloculata* (green). (e) Sea water $\delta^{18}$O ($\delta^{18}O_{sw}$, pink). (f) The difference between SST and TWT ($\Delta T_{G\text{-}P}$, grey). The thicker lines in these time-series represent the five point average of the original data (thin lines). (g) AMS $^{14}$C dates (crosses) and mean sedimentation rates (solid line). The five stages mentioned in text are divided by vertical dashed lines.

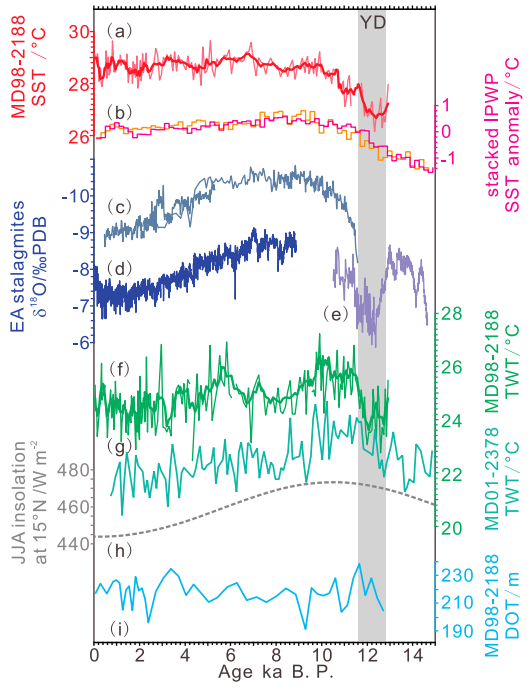


**Figure 3.** Comparison of Holocene climate changes in IPWP and East Asia. (a) MD98-2188 SST (in red, this study), and (b) the stacked Holocene SST variability in IPWP (orange and carmine) [*Linsley et al.*, 2010]. (c) Sanbao (navy), (d) Dongge (blue), and (e) Hulu (indigo) stalagmite $\delta^{18}O$ records from Southeast China [*Wang et al.*, 2001, 2005, 2008]. TWT from (f) MD98-2188 (green, this study) and (g) MD01-2378 (aqua) [*Xu et al.*, 2008]. (h) The summer (JJA) insolation at 15°N (grey) computed by La2004 [*Laskar et al.*, 2004]. (i) DOT estimated from planktonic foraminifera transfer function (cyan, data from *Lin et al.* [2006] using the method of *Andreasen and Ravelo*, [1997]). The time interval of the Younger Dryas event (YD) is denoted by the grey bar.

beneath the mixed layer, respectively [e.g., *Xu et al.*, 2006]. In the top 10 cm of core MD98-2188 (5 samples, none older than 200 yr), the average $\delta^{18}O$ and Mg/Ca for *G. ruber* yield values of −3.00‰ ± 0.17‰ and 5.11 ± 0.18 mmol/mol, and for *P. obliquiloculata* of −1.54‰ ± 0.12‰ and 2.91 ± 0.17 mmol/mol. These values agree well with estimates by sediment traps in IPWP of 0–50 m ($\delta^{18}O$ = −2.5∼−3.5‰, Mg/Ca = 4∼6 mmol/mol) and 100–150 m water depth ($\delta^{18}O$ = −1.5∼–2.5‰, Mg/Ca = 2.4∼3.4 mmol/mol) [*Kawahata et al.*, 2002; *Mohtadi et al.*, 2009].

## 4. Results

[13] The measured $\delta^{18}O$ variations span a range of ∼2‰ for both *G. ruber* (−1∼−3‰PDB) and *P. obliquiloculata* (0∼−2‰PDB) and show a consistent decrease between ∼13 and ∼9 ka (Figures 2a and 2b). The overall amplitudes of estimated change, ∼3°C, were also similar for both SST (26∼29°C) and TWT (23∼26°C) (Figures 2c and 2d). The calculated $\delta^{18}O_{sw}$ displays a long-term decrease by ∼0.4‰ through the Holocene (Figure 2e).

[14] Based mainly on variations in TWT, records in MD98-2188 (Figure 2) can be characterized by five distinct stages: (I) 13∼12 ka, SST and TWT were respectively ∼1.7°C and ∼1.0°C lower than their Holocene mean value; (II) 12∼10 ka, TWT increased quickly within no more than 400 yrs to a distinct peak (∼1.5°C higher than the late Holocene) around ∼11.5 ka that lasted for ∼1500 yrs, while SST increased gradually and $\Delta T_{G\text{-}P}$ was at a minimum (Figure 2f); (III) 10∼6 ka, both SST and TWT maintained roughly constant while TWT was ∼0.6°C lower than the previous stage; (IV) 6∼3 ka, TWT reached another minor peak around 5.6 ka and then decreased by ∼0.7°C to 3 ka; (V) 3∼0 ka, all proxies remained roughly constant except for some superimposed sub-millennial fluctuations.

## 5. Discussion

[15] The reconstructed Holocene SST (Figure 3a) and $\delta^{18}O_{sw}$ (Figure 2e) variations in MD98-2188 are in good agreement with other records from the IPWP (Figure 3b) [e.g., *Lea et al.*, 2000; *Stott et al.*, 2004; *Linsley et al.*, 2010]; while the TWT variability in MD98-2188 (Figure 3f) is also in accordance with another *P. obliquiloculata* Mg/Ca reconstruction (Figure 3g) from the southwest IPWP (core MD2378, see Figure 1a for its location [*Xu et al.*, 2008]) despite a ∼2°C difference between the two throughout the Holocene. Thus, it may be inferred that the Holocene SST and TWT records in MD98-2188 were coherent with and could characterize the observed changes over the IPWP.

[16] Obviously, there were prominent differences between the SST and TWT changes. After the interval of YD, a distinct peak was reached in TWT between ∼12 and ∼10 ka (∼1.5°C warmer than the late Holocene average; Figures 3f and 3g). This early Holocene TWT peak agrees well with the timing of the Holocene maximum in boreal summer insolation between ∼13 and ∼9 ka (Figure 3h). During the remainder of the Holocene, the subsequent decline in IPWP TWT at both sites MD98-2188 and MD01-2378 was larger than 1°C. In contrast, the SST in the IPWP appears to show an Early Holocene Optimum between 10∼7 ka with temperatures no more than 0.5°C higher than the late Holocene [*Stott et al.*, 2004; *Linsley et al.*, 2010] (Figures 3a and 3b). Reconstructed SSTs in these studies lag the boreal summer insolation maximum by ∼3 ka and show a much smaller Holocene decrease. Accordingly, we argue that, rather than SST, the response of the IPWP to the solar insolation forcing in the Holocene could be characterized by subsurface temperature changes and resultant upper-ocean heat content modulations.

[17] *Xu et al.* [2008] had interpreted the Holocene TWT cooling in MD01-2378 to represent intensifications of "cool thermocline-dominated Indonesian Throughflow (ITF)" and attribute the initiation of such changes to the continuous sea level rise around ∼9 ka. Given the similar TWT variability in MD98-2188, circulation reformations may occur not only within ITF, but throughout the IPWP, for acquiring the coherent TWT changes within this region. Accordingly, more processes may have been involved besides sea level change.

[18] Though one might expect either changes in the thermocline water or/and motions of the depth of thermocline (DOT) as causes for the Holocene TWT (Figures 3f and 3g) and the subsequent $\Delta T_{G\text{-}P}$ (Figure 2f) variability, the estimated DOT for core MD98-2188 using the transfer function of *Andreasen and Ravelo* [1997] barely changed in its trend

from Early to Late Holocene (Figure 3i, planktonic assemblage data courtesy of *Lin et al.* [2006]). Therefore, without further evidence, one would tend to take changes within the IPWP thermocline water as a major cause for the TWT variability, which implied lateral heat/water advection within the subsurface.

[19] In terms of the subsurface lateral advection, a first approximation of the plausible mechanisms for a boreal summer insolation driving on the IPWP TWT could lie in that the flux and temperature of the NPTW flowing to the low-latitude western Pacific are mediated by the evaporation-induced subduction of near-surface water in the central Subtropical Pacific [e.g., *Fine et al.*, 1994], which could be controlled effectively by radiation heating.

[20] At the regional point of view, the TWT changes in IPWP could be connected to the southward movement of the ITCZ in the Holocene [e.g., *Haug et al.*, 2001; *Wang et al.*, 2005] (Figures 3c–3e), potentially through the modulation effect of the ITCZ-generated basin-interior barrier on the flux of the thermocline ventilation to the western boundary [e.g., *Lu and McCreary*, 1995] besides the commonly shared insolation forcing. While ITCZ were moving more southerly through the Holocene, the basin-interior barrier could be less energized, thereby less NPTW would be transported to the western boundary, favoring the cooling in IPWP's TWT.

[21] From a local point of view, the NECB may have moved in the past due to changes in the regional winds, thus influenced TWT near site MD98-2188 and downstream the Mindanao Current and ITF. During the TWT warming that marked the end of YD, the NECB may have relocated southward because of the strengthening of EASM [e.g., *Wang et al.*, 2001] (Figure 3e), the weakening of EAWM [e.g., *Huang et al.*, 2011], and the weakening of the trade winds owing to the northward return of ITCZ [e.g., *Haug et al.*, 2001; *Wang et al.*, 2001]. This could have favored the early Holocene TWT peak by strengthening the input of warmer NPTW. The opposite processes, i.e. slow weakening of the EASM and southward moving of the ITCZ [*Wang et al.*, 2005; *Haug et al.*, 2001], may have occurred through the Holocene and benefit the TWT cooling by weakening the input of NPTW. Furthermore, the minor TWT spike around ~6 ka and the following cooling till 3 ka might be linked to the weakening and re-strengthening of El Niño and Southern Oscillation in the Mid-Holocene [e.g. *Rein et al.*, 2005] through the alteration of the tropical trade-wind intensity [e.g., *Qu and Lukas*, 2003; *Kim et al.*, 2004].

## 6. Concluding Remarks

[22] Planktonic foraminiferal Mg/Ca-derived SST and TWT in the western tropical Pacific behavior differently through the Holocene and suggest differences in their response to insolation forcing and correlations to low-latitude climate changes. The thermocline in the IPWP is shown to be a vigorous component of the climate system for its feedback to boreal summer insolation and its interactions with tropical climate.

[23] **Acknowledgments.** This work was supported by funds to Z. Jian (National Natural Science Foundation of China 91028004 and 41023004). The authors appreciate the generous data-sharing of Yu-Shih Lin and Jian Xu, and the critical and constructive reviews on the manuscripts by Larry Peterson and other anonymous reviewers.

[24] The Editor thanks two anonymous reviewers for their assistance in evaluating this paper.

## References

Anand, P., H. Elderfield, and M. C. Conte (2003), Calibration of Mg/Ca thermometry in planktonic foraminifera from a sediment trap time series, *Paleoceanography*, *18*(2), 1050, doi:10.1029/2002PA000846.

Andreasen, D. J., and A. C. Ravelo (1997), Tropical Pacific Ocean thermocline depth reconstructions for the Last Glacial Maximum, *Paleoceanography*, *12*, 395–413, doi:10.1029/97PA00822.

Antonov, J. I., D. Seidov, T. P. Boyer, R. A. Locarnini, A. V. Mishonov, and H. E. Garcia (2010), *World Ocean Atlas 2009*, vol. 2, *Salinity*, edited by S. Levitus, *NOAA Atlas NESDIS*, vol. 69, NOAA, Silver Spring, Md.

Bemis, B. E., H. J. Spero, J. Bijma, and D. W. Lea (1998), Reevaluation of the oxygen isotopic composition of planktonic foraminifera: Experimental results and revised paleotemperature equations, *Paleoceanography*, *13*, 150–160, doi:10.1029/98PA00070.

Chen, D., A. J. Busalacchi, and L. M. Rothstein, (1994), The roles of vertical mixing, solar radiation, and wind stress in a model simulation of the sea surface temperature seasonal cycle in the tropical Pacific Ocean, *J. Geophys. Res.*, *99*, 20,345–20,359.

Cheng, X., B. Huang, Z. Jian, Q. Zhao, J. Tian, and J. Li (2005), Foraminiferal isotopic evidence for monsoonal activity in the South China Sea: A present-LGM comparison, *Mar. Micropaleontol.*, *54*, 125–139, doi:10.1016/j.marmicro.2004.09.007.

Fine, R. A., R. Lukas, F. M. Bingham, M. J. Warner, and R. H. Gammon (1994), The western equatorial Pacific: A water mass crossroad, *J. Geophys. Res.*, *99*, 25,063–25,080, doi:10.1029/94JC02277.

Fine, R. A., K. A. Maillet, K. F. Sullivan, and D. Willey (2001), Circulation and ventilation flux of the Pacific Ocean, *J. Geophys. Res.*, *106*, 22,159–22,178, doi:10.1029/1999JC000184.

Harper, S. (2000), Thermocline ventilation and pathways of tropical-subtropical water mass exchange, *Tellus, Ser. A*, *52*, 330–345.

Haug, G. H., K. A. Hughen, D. M. Sigman, L. C. Peterson, and U. Rohl (2001), Southward migration of the Intertropical Convergence Zone through the Holocene, *Science*, *293*, 1304–1308, doi:10.1126/science.1059725.

Huang, B., and Z. Liu (1999), Pacific subtropical-tropical thermocline water exchange in the National Centers for Environmental Prediction ocean model, *J. Geophys. Res.*, *104*, 11,065–11,076, doi:10.1029/1999JC900024.

Huang, E., J. Tian, and S. Steinke (2011), Millennial-scale dynamics of the winter cold tongue in the southern South China Sea over the past 26 ka and the East Asian winter monsoon, *Quat. Res.*, *75*, 196–204, doi:10.1016/j.yqres.2010.08.014.

Kawahata, H., A. Nishimura, and M. K. Gagan (2002), Seasonal changes in foraminiferal production in the western equatorial Pacific warm pool: Evidence from sediment trap experiments, *Deep Sea Res., Part II*, *49*, 2783–2800, doi:10.1016/S0967-0645(02)00058-9.

Kim, Y. Y., T. Qu, T. Jensen, T. Miyama, H. Mitsudera, H.-W. Kang, and A. Ishida (2004), Seasonal and interannual variations of the North Equatorial Current bifurcation in a high-resolution OGCM, *J. Geophys. Res.*, *109*, C03040, doi:10.1029/2003JC002013.

Laskar, J., P. Robutel, F. Joutel, M. Gastineau, A. C. M. Correia, and B. Levrard (2004), A long term numerical solution for the insolation quantities of the Earth, *Astron. Astrophys.*, *428*, 261–285, doi:10.1051/0004-6361:20041335.

Lea, D. W., D. K. Pak, and H. J. Spero (2000), Climate impact of late Quaternary equatorial Pacific sea surface temperature variations, *Science*, *289*, 1719–1724, doi:10.1126/science.289.5485.1719.

Lin, Y.-S., K.-Y. Wei, I.-T. Lin, P.-S. Yu, H.-W. Chiang, C.-Y. Chen, C.-C. Shen, H.-S. Mii, and Y.-G. Chen (2006), The Holocene Pulleniatina minimum event revisited: Geochemical and faunal evidence from the Okinawa Trough and the upper reaches of the Kuroshio Current, *Mar. Micropaleontol.*, *59*, 153–170, doi:10.1016/j.marmicro.2006.02.003.

Linsley, B. K., Y. Rosenthal, and D. W. Oppo (2010), Holocene evolution of the Indonesian Throughflow and the western Pacific warm pool, *Nat. Geosci.*, *3*, 578–583, doi:10.1038/ngeo920.

Liu, Z., S. G. H. Philander, and R. C. Pacanowski (1994), A GCM study of tropical-subtropical upper-ocean water exchange, *J. Phys. Oceanogr.*, *24*, 2606–2623, doi:10.1175/1520-0485(1994)024<2606:AGSOTU>2.0.CO;2.

Locarnini, R. A., A. V. Mishonov, J. I. Antonov, T. P. Boyer, and H. E. Garcia (2010), *World Ocean Atlas 2009*, vol. 1, *Temperature*, edited by S. Levitus, *NOAA Atlas NESDIS*, vol. 68, NOAA, Silver Spring, Md.

Lu, P., and J. P. McCreary (1995), Influence of the ITCZ on the flow of thermocline water from the subtropical to the equatorial Pacific Ocean, *J. Phys. Oceanogr.*, *25*, 3076–3088, doi:10.1175/1520-0485(1995)025<3076:IOTIOT>2.0.CO;2.

Luyten, J. R., J. Pedlosky, and H. Stommel (1983), The ventilated thermocline, *J. Phys. Oceanogr.*, *13*, 292–309, doi:10.1175/1520-0485(1983)013<0292:TVT>2.0.CO;2.

Martin, P. A., and D. W. Lea (2002), A simple evaluation of cleaning procedures on fossil benthic foraminiferal Mg/Ca, *Geochem. Geophys. Geosyst.*, *3*(10), 8401, doi:10.1029/2001GC000280.

Mohtadi, M., S. Steinke, J. Groeneveld, H. G. Fink, T. Rixen, D. Hebbeln, B. Donner, and B. Herunadi (2009), Low-latitude control on seasonal and interannual changes in planktonic foraminiferal flux and shell geochemistry off south Java: A sediment trap study, *Paleoceanography*, *24*, PA1201, doi:10.1029/2008PA001636.

Qu, T., and R. Lukas (2003), The bifurcation of the North Equatorial Current in the Pacific, *J. Phys. Oceanogr.*, *33*, 5–18, doi:10.1175/1520-0485(2003)033<0005:TBOTNE>2.0.CO;2.

Qu, T., H. Mitsudera, and T. Yamagata (1999), A climatology of the circulation and water mass distribution near the Philippine coast, *J. Phys. Oceanogr.*, *29*, 1488–1505, doi:10.1175/1520-0485(1999)029<1488:ACOTCA>2.0.CO;2.

Rein, B., A. Lückge, L. Reinhardt, F. Sirocko, A. Wolf, and W.-C. Dullo (2005), El Niño variability off Peru during the last 20,000 years, *Paleoceanography*, *20*, PA4003, doi:10.1029/2004PA001099.

Rosenthal, Y., et al. (2004), Interlaboratory comparison study of Mg/Ca and Sr/Ca measurements in planktonic foraminifera for paleoceanographic research, *Geochem. Geophys. Geosyst.*, *5*, Q04D09, doi:10.1029/2003GC000650.

Seager, R., and R. Murtugudde (1997), Ocean dynamics, thermocline adjustment, and regulation of topical SST, *J. Clim.*, *10*, 521–534, doi:10.1175/1520-0442(1997)010<0521:ODTAAR>2.0.CO;2.

Stott, L., K. Cannariato, R. Thunell, G. H. Haug, A. Koutavas, and S. Lund (2004), Decline of surface temperature and salinity in the western tropical Pacific Ocean in the Holocene epoch, *Nature*, *431*, 56–59, doi:10.1038/nature02903.

Stuiver, M., and P. J. Reimer (1993), Extended $^{14}$C database and revised CALIB radiocarbon calibration program, *Radiocarbon*, *35*, 215–230.

Waelbroeck, C., L. Labeyrie, E. Michel, J. C. Duplessy, J. F. McManus, K. Lambeck, E. Balbon, and M. Labracherie (2002), Sea-level and deep water temperature changes derived from benthic foraminifera isotopic records, *Quat. Sci. Rev.*, *21*, 295–305, doi:10.1016/S0277-3791(01)00101-9.

Wang, Y., H. Cheng, R. L. Edwards, Z. An, J. Wu, C. Shen, and J. A. Dorale (2001), A high-resolution absolute-dated Late Pleistocene monsoon record from Hulu Cave, China, *Science*, *294*, 2345–2348, doi:10.1126/science.1064618.

Wang, Y., H. Cheng, R. L. Edwards, Y. He, X. Kong, Z. An, J. Wu, M. J. Kelly, C. A. Dykoski, and X. Li (2005), The Holocene Asian monsoon: Links to solar changes and North Atlantic climate, *Science*, *308*, 854–857, doi:10.1126/science.1106296.

Wang, Y., H. Cheng, R. L. Edwards, X. Kong, X. Shao, S. Chen, J. Wu, X. Jiang, X. Wang, and Z. An (2008), Millennial- and orbital-scale changes in the East Asian monsoon over the past 224,000 years, *Nature*, *451*, 1090–1093, doi:10.1038/nature06692.

Xu, J., W. Kuhnt, A. Holbourn, N. Andersen, and G. Bartoli (2006), Changes in the vertical profile of the Indonesian Throughflow during Termination II: Evidence from the Timor Sea, *Paleoceanography*, *21*, PA4202, doi:10.1029/2006PA001278.

Xu, J., A. Holbourn, W. Kuhnt, Z. Jian, and H. Kawamura (2008), Changes in the thermocline structure of the Indonesian outflow during Termination I and II, *Earth Planet. Sci. Lett.*, *273*, 152–162, doi:10.1016/j.epsl.2008.06.029.

F. Bassinot, Laboratoire des Science du Climat et de l'Environnement, Domaine du CNRS, Gif-sur-Yvette F-91198, France.

X. Cheng, H. Dang, Z. Jian, and P. Qiao, State Key Laboratory of Marine Geology, Tongji University, Shanghai 200092, China. (hwdang@gmail.com)